Neural Computing and Applications
https://doi.org/10.1007/s00521-018-03992-y

ORIGINAL ARTICLE

Anatomical connectivity changes in bipolar disorder and schizophrenia investigated using whole-brain tract-based spatial statistics and machine learning approaches

Bernis Sutcubasi[1] · Sinem Zeynep Metin[2] · Turker Tekin Erguzel[3] · Baris Metin[1] · Cumhur Tas[1] · Mehmet Kemal Arikan[1] · Nevzat Tarhan[2]

Received: 31 January 2018 / Accepted: 31 December 2018

Abstract
Schizophrenia and bipolar disorder have similar clinical features. Their differential diagnosis is crucial because each has different prognostic and therapeutic characteristics. Earlier studies have used numerous methods, including magnetic resonance investigation, in an effort to differentiate these two disorders. Research has consistently shown that there is reduced white matter density in the fronto-temporal and fronto-thalamic pathways in both patients with bipolar disorder and schizophrenia; however, the sensitivity of the methods used is limited. Tract-based spatial statistics is a method of whole-brain analysis that relies on voxel-based comparison, and uses nonlinear image transformation and permutation tests with correction for multiple comparisons. The primary aim of the present study was to investigate anatomical connectivity changes in patients with bipolar disorder and schizophrenia using tract-based spatial statistics, to classify the patients according to white matter integrity patterns using machine learning, and to identify features that represent the key differences between the disorders. Whole-brain images of 41 bipolar disorder patients, 39 schizophrenia patients, and 23 controls were acquired using a 1.5 T magnetic resonance investigation scanner. As compared to the controls, the schizophrenia and bipolar disorder patients had reduced fractional anisotropy in similar white matter tracts. In addition, the imaging method employed differentiated the schizophrenia and bipolar disorder patients with 81.25% accuracy. Although the bipolar disorder and schizophrenia patients exhibited similar anatomical connectivity changes, as compared to the controls, the connectivity reductions in the right hemisphere in the bipolar disorder patients differentiated them from the schizophrenia patients. The present findings improve our understanding of the etiology and pathogenesis of bipolar disorder and schizophrenia, and can potentially be used as a biomarker for the diagnosis and treatment of both disorders.

Keywords Bipolar disorder · Schizophrenia · Tract-based spatial statistics · Machine learning

1 Introduction

Bipolar disorder (BD) is a psychiatric disorder characterized by episodes of mania and depression. During a manic episode, individuals often have excessive energy, and move, think, and speak rapidly. They can also experience delusions and suspect that others seek to harm them. During a manic episode, some individuals have visual and/or auditory hallucinations. Episodes of severe depression and dysfunctions in several cognitive areas also occur in individuals with BD [1]. Schizophrenia (SCH) is a psychiatric disorder characterized by a group of so-called positive symptoms, including hallucinations, delusions, and/or disordered thought. Individuals with SCH can also

✉ Baris Metin
baris.metin@uskudar.edu.tr

[1] Department of Psychology, Faculty of Humanities and Social Sciences, Uskudar University, Haluk Turksoy sok. No:14, Altunizade, Uskudar, Istanbul, Turkey

[2] Psychiatry Unit, NPIstanbul Hospital, Uskudar University, Istanbul, Turkey

[3] Department of Computer Engineering, Faculty of Engineering and Natural Sciences, Uskudar University, Istanbul, Turkey

Published online: 12 January 2019

have negative symptoms, such as diminished social interaction, lack of pleasure in previously enjoyable activities, diminished speech, and an effect lacking expressiveness. As can be seen, the positive symptoms of SCH can mimic a BD manic episode, and the negative symptoms of SCH can be similar to those of a BD depressive episode, and psychiatrists often see both patients with a mixture of positive and negative symptoms. Furthermore, antipsychotics are used to treat both disorders [2], cognitive deficits are common in both [3], the genetic risk factors are similar for both [4], and abnormalities in the neurotransmitter system [5, 6] are observed in both SCH and BD. In addition, up to 75% of first-episode SCH patients exhibit symptoms of depression [7]. Based on the similarities in the clinical presentation of SCH and BD, it can be difficult to accurately diagnose both according to clinical findings only [8].

These similarities led to a search for biomarkers that can differentiate between the two disorders when initial symptoms appear. Neuroimaging is a method that can yield specific and sensitive biomarkers, and diffusion tensor imaging (DTI) facilitates detection of microstructural alterations in white matter tracts. Furthermore, a limited number of studies showed that, as compared to healthy controls, BD patients have lower fractional anisotropy (FA) in the following regions (for a review see [9]): the anterior thalamic radiation and uncinate fasciculus, the fornix, posterior cingulate, corpus callosum, and parietal and temporal corona radiate [10, 11]. Additionally, Versace et al. [12] observed higher FA in the frontal cortex, temporal cortex, cuneus, and left uncinate fasciculus in BD patients than in healthy controls. In contrast, whole-brain analysis using tract-based spatial statistics (TBSS) shows that patients with SCH have lower FA in the inferior and superior longitudinal fasciculus, superior and left inferior fronto-occipital fasciculus, corpus callosum, anterior thalamic radiation, posterior corona radiate, and uncinate fasciculus, as compared to healthy controls [13–16]. In addition, higher FA was observed in the inferior part of the corticopontine–cerebellar circuit in SCH patients than in healthy controls [13].

To date, few studies directly compared white matter tracts in SCH and BD patients [e.g., 17]. Those that did reported similar structural brain abnormalities in patients with both disorders, including reduced white matter density in the fronto-temporal and fronto-thalamic pathways, such as the anterior internal capsule and uncinate fasciculus, as compared to controls. Only one study noted a significant difference between SCH and BD: Lu et al. [18] reported that individuals with BD had lower FA in the posterior thalamic radiation and inferior longitudinal fasciculus than SCH patients.

One reason the studies above observed few differences between SCH and BD patients is that all used standard registration and smoothing procedures, followed by voxel-based analysis, and the arbitrary choice of smoothness [19] and alignment inaccuracies [20] limit generalizability of the data [21]. TBSS is a whole-brain voxel-based analysis method that provides sophisticated solutions to smoothness and alignment problems when evaluating white matter alterations [21]. TBSS, which uses nonlinear image transformation and permutation tests, with correction of multiple comparisons, does not require smoothing. The primary aim of the present study was to determine white matter differences in SCH and BD patients that could be used for accurate differential diagnosis. The present study used TBSS and machine learning (ML) to investigate the differences between SCH and BD patients.

As earlier studies showed overlapping white matter alterations in both disorders, it was hypothesized that SCH and BD patients would exhibit similar structural brain abnormalities, as compared to healthy controls. In addition, it was hypothesized that it would be possible to accurately differentiate SCH and BD patients based on white matter tract FA values. As such, a secondary aim of the present study was to discern the pathophysiological differences between BD and SCH patients. Furthermore, multiple ML approaches were compared to determine which could be a potential diagnostic tool for differentiating BD and SCH patients.

2 Materials and methods

2.1 Participants

The study included 103 participants: 39 in the SCH group, 41 in the BD, and 23 in the control group. Patients were administered a structured interview and diagnosed based on DSM-IV and the consensus of two psychiatrists. The SCH group included 27 males and 12 females aged 14–74 years (mean age 31.15 $\pm$ 12.09 years), and the BD group included 23 males and 18 females aged 15–60 years (mean age 33.51 $\pm$ 10.13 years). The control group included 14 males and 9 females aged 20–45 years (mean age 30.52 $\pm$ 6.50 years) with a negative history of neurological and psychiatric disease. The study protocol was approved by the Uskudar University Ethics Committee. The control group provided written informed consent. However, the SCH and BD patients were identified retrospectively based on hospital records, and therefore, informed consent was not obtained.

2.2 Data acquisition

Whole-brain images were acquired at NP Istanbul-Uskudar University, Istanbul, Turkey, using a 1.5 Tesla Philips

Achieva MRI scanner (Philips Medical Systems, Best, the Netherlands) and a SENSE eight-channel head coil. All DTI sequences were based on a single-shot spin-echo echo-planar imaging (EPI) sequence. The imaging parameters were as follows: repetition time (TR): 9024.51 ms; echo time (TE): 66.752 ms; acquisition matrix: 128 × 128; flip angle: 90°; voxel size: 1.75 mm × 1.75 mm × 2 mm; slice thickness: 2 mm; slice spacing: 2 mm. One b0 image without diffusion weighting and 16 non-collinear gradient directions were acquired with a single b value of 800 s mm^{-2}.

2.3 Image processing

This study used TBSS for whole-brain analysis (TBSS version 1.0, FMRIB Center, Oxford, UK [21] (TBSS is a software package implemented in FSL version 5.0 software [FMRIB Software Library, http://www.fmrib.ox.ac.uk/fsl/] [22]). Eddy current correction was used for standard pre-processing including motion correction and, with co-registration to the B0 image with gradient directions corrected. Following eddy current correction, brain extraction was implemented using Brain Extraction Tool (BET) [23] and the diffusion tensor was calculated using the DTIFIT program to create a single FA image for each participant. The standard TBSS procedure was used for the remainder of the analyses [21]. All individual FA volumes were registered to the FMRIB58 template using nonlinear registration. Then, the nonlinearly aligned images are merged into a single 4D image file and the mean of all FA images was calculated. All individual FA data were thinned to generate a mean FA skeleton. FA values for all white matter tracts in each participant, based on the JHU White Matter Tractography Atlas [24], were calculated using ROIs, as follows: 20 ROIs were created on the mean FA skeleton, and FA values for each participant's mean-aligned image were extracted for each skeletal region. Thus, average FA values for all tracts were obtained and used for ML-based classification.

2.4 Machine learning classification

Following ROI data extraction, the support vector machine (SVM) approach and artificial neural network (ANN) approach were used to differentiate the SCH or BD patients. (Detailed information about the ANN and the genetic algorithm [GA] is given in Appendices 1 and 2.) Additionally, a feature selection process and imported GA were used to generate a hybrid structure, as previously described [17, 23, 24]. In order to reduce the number of features given as the input matrix to the model and to ensure the more informative features, GA was employed in a wrapper-based fashion. GA was implemented using a population of 150, a two-point crossover probability of 0.5, and a mutation rate of 0.1. At each step, the GA uses the current population that is representing the whole solution set, to create the children that make up the next generation. Crossover and mutation were applied uniformly to each generation's selected individuals. As the individuals that tend to have a higher probability of survival are valuable for the feature selection process, they are expected to go forward to form the new generation. The selection scheme used tournament size as 0.2 that specifies the fraction of the current population which should be used as tournament members.

In order to eliminate overfitting, it is widely used to hold out some part of the data as a test set when performing a supervised learning experiment, such as ANN. Through the calculation process of "hyperparameters" for the predictive models, there is still a risk of overfitting on the test set since the parameters could be tweaked until the estimator performs optimally. Therefore, the information could "leak" into the model and the evaluation metrics then no longer report on generalization performance. In order to solve that problem, whole data were divided into three parts. Firstly, 70% of the data are processed as training set, while the remaining data are divided into equal-sized "validation set" and "test set." The training subset was first employed in order to fit the models, and the validation set was then employed to estimate prediction error for model selection. Finally, the test set was used for assessment of the generalization error of the final chosen model. Since splitting the data into three separate sets, we drastically reduce the number of sample sets, which could be used for learning the model, and the results could depend on a particular random choice for train, validation sets. A valuable solution to this problem is cross-validation (CV). Basically, with k-fold CV the whole dataset is employed efficiently. A test set is still held out for the final evaluation, but the validation set is no longer needed for CV. The training dataset is divided into k smaller sets, the model is trained using k-1 of the folds as training data, and then, the resulting model is validated on the remaining data to compute a performance measure such as accuracy. This approach could be computationally expensive, but values the dataset are very small. In this study, fourfold CV with stratified sampling was used. To compare the performance of ANN, SVM models were also created using the datasets. In order to compare the performance of the aforementioned methods, three measures were used: (1) overall accuracy; (2) area under the ROC curve (AUC) value; and (3) Gini coefficient. The Gini coefficient can be generated directly from the AUC value, which is the ratio of the area between the ROC curve and the diagonal line to the area of the above triangle in the ROC curve. Gini = (2*AUC − 1) is

the equation used to express the Gini coefficient in terms of the AUC value.

2.5 Statistical analysis

One-way ANOVA and the Chi-square test were used to compare age and gender variables between the three groups. Statistical analyses were performed using Statistical Package for the Social Sciences (SPSS 22), and $P < 0.05$ was used for statistical significance.

3 Results

There were not any significant differences in age ($t(100) = 0.811$, $P = 0.447$; see Table 1) or gender (χ^2 (1, $n = 103$) = 1.48, $P = 0.48$) between the SCH, BD, and control groups.

The classification performance of the SVM and ANN models is shown in Table 2. The performance of the ANN approach was better than that of the SVM model, but not satisfactory. This finding shows that the ANN-GA model using five white matter tracts (the right inferior fronto-occipital fasciculus, right inferior longitudinal fasciculus, right hippocampus, the temporal part of the right superior longitudinal fasciculus, and the forceps major) outperformed the other model. Moreover, with fewer features the ANN-GA model generated a remarkable AUC value. The Gini coefficient also indicates that it performed better than standalone SVM and ANN models.

As given in Table 2, ANN and SVM approaches were employed, respectively, in order to compare their classification capability. Since ANN outperformed, GA step is added to the model to boost the performance of the system. In addition to the increasing performance of the hybrid model, less number of features, 5 of 20, was fed into the model.

Table 3 gives the classification outcome of the model. In total, 36 of 41 SCH subjects and 29 of 39 BD subjects were correctly classified, resulting in 81.25 overall classification accuracy that is quite satisfactory.

Figure 1 shows that the performance of the ANN-GA hybrid model was better and had remarkable predictive generalization capability, with a higher true positive rate and lower false positive FP rate that underlines a high area under curve value.

As compared to the controls, the SCH patients (Fig. 2) and BD patients (Fig. 3) had lower FA in several white matter tracts (see Table 4); however, as shown in Table 4, the age range in the patient groups was wider. In order to eliminate errors due to the difference in age range, individuals were removed from the patient groups to make the age range equal to that in the control group; however, even after limiting the age range in the SCH and BD groups, the results remained consistent (Table 4).

Table 1 Demographic findings according to group

Group	Age (years)		Gender (*n*)	
	Mean	SD	Female	Male
BP	33.51	10.13	18	23
SCH	31.15	12.09	12	27
Control	30.52	6.501	9	14

4 Discussion

The present study used voxel-based TBSS and ML methods to determine whether FA values could be used to differentiate BD and SCH patients. The TBSS results demonstrate that the SCH and BD groups lower FA reductions in similar white matter tracts, as compared to the control group. Furthermore, the decrease in FA in the BD group was more pronounced in white matter tracts in the right hemisphere, as compared to SCH group, and the ANN-GA method accurately differentiated the participants with 81.25% accuracy.

The present findings have a number of implications. The findings show that BD patients have lower FA in the right hemisphere white matter tracts (the inferior fronto-occipital fasciculus, inferior longitudinal fasciculus, hippocampus, and the temporal part of the superior longitudinal fasciculus) and in the forceps major than SCH patients. The inferior fronto-occipital fasciculus connects the occipital cortex to the orbitofrontal regions and passes through the temporal lobe and insula. Additionally, it is known to play a crucial role in identification of facial emotion [25], visuospatial processing [26], and semantic processing [27]. Earlier studies reported abnormal fronto-occipital connectivity in patients with BD, obsessive–compulsive disorder, and psychotic symptoms [28–30]. In the present study, low FA was observed only in the right inferior fronto-occipital fasciculus in the BD group. The inferior longitudinal fasciculus connects the white matter tracts in the anterior temporal lobe and amygdala to the prefrontal cortex and other cortical regions [31]. Recent findings show that the inferior longitudinal fasciculus plays a key role in visual-specific semantic memory and emotion processing [32, 33]. In BD patients, lower FA in the inferior fronto-occipital fasciculus and inferior longitudinal fasciculus might be associated with impaired visual processing or emotion dysregulation [34]. The hippocampus is part of the Papez circuit and is involved in emotional regulation [35]. Although most of the structural imaging studies reviewed

Table 2 Classification performance of ANN models for FA values in white matter tracts

Models	Overall accuracy (%)	Number of features	AUC value	Gini
SVM	58.75	20	0.61	0.22
ANN	65	20	0.68	0.36
ANN-GA	81.25	5	0.83	0.66

Table 3 Classification performance of GA-ANN approach

	Real SCH	Real BD
Prediction of SCH	36	10
Prediction of BD	5	29
Accuracy	81.25%	

did not report any hippocampal alterations in BD patients (see Frey et al. [36] for a review), a few reported that right hippocampal volume was smaller in BD patients than in healthy controls [37]. It was also compared psychotic and non-psychotic BD patients, SCH patients, and controls, and observed smaller left hippocampal volume in the non-psychotic BD patients, as compared to the controls; however, they did not note any difference between the psychotic and non-psychotic BD and SCH patients. The superior longitudinal fasciculus connects the white matter tracts in the frontal association cortices to the temporo-parietal regions and plays a role in auditory and speech processing and visuospatial attention [38, 39]. It was reported that disruption of the superior longitudinal fasciculus pathway is associated with the positive symptoms of

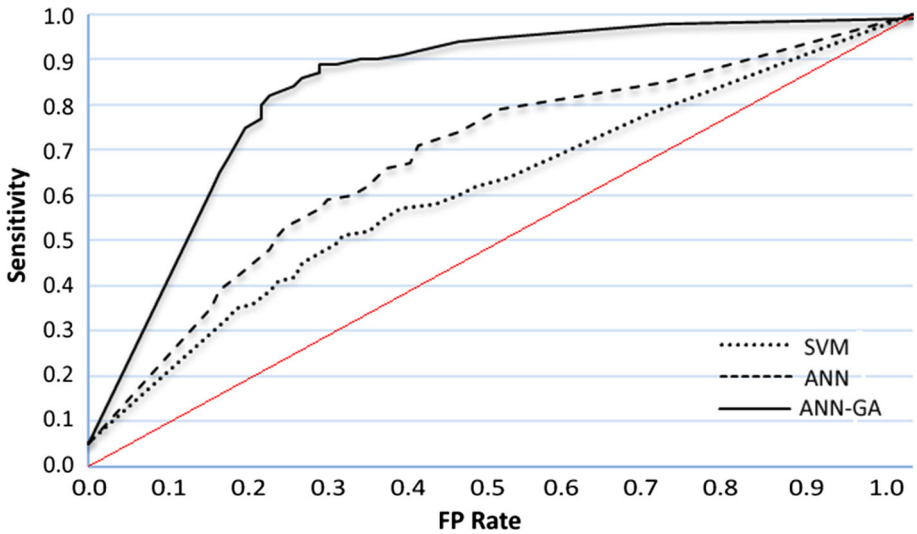

Fig. 1 ROC curves for the SVM, ANN, and ANN-GA models

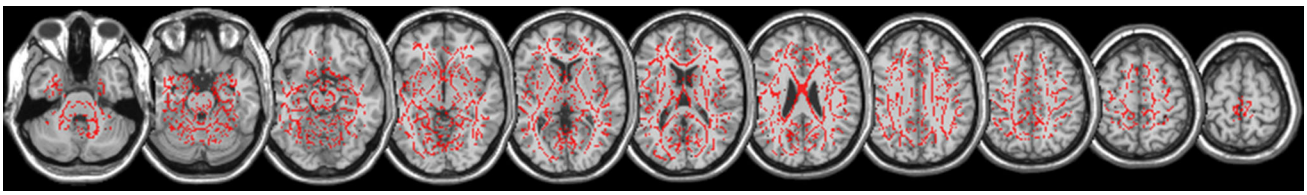

Fig. 2 White matter tracts showing significantly lower FA values in patients with SCH than HC

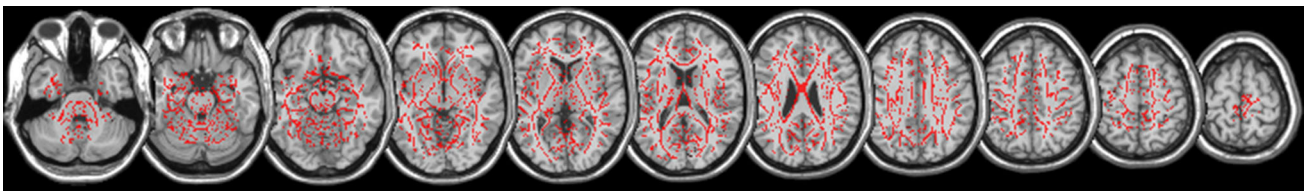

Fig. 3 White matter tracts showing significantly lower FA values in patients with BD than HC

Table 4 Clusters showing significantly lower FA values in the SCH and BD patients, as compared to age-matched controls

Contrast	Voxels	*P* value	Max *X* (mm)	Max *Y* (mm)	Max *Z* (mm)	Peak difference
C > SCH (age-matched)	171,480	1	7	− 33	− 42	Corticospinal tract
C > BD (age-matched)	169,969	1	13	− 35	− 39	Corticospinal tract

TFCE-corrected results, $P < 0.001$

BD [10]. In the present study, low FA in the temporal part of the right superior longitudinal fasciculus was observed in BD patients; the clinical correlate of these findings should be explored in the future. The forceps major connects the occipital lobes to the corpus callosum, and an earlier study reported that the FA value in the forceps major correlates with psychotropic medication load in BD patients [40]. The present findings, low FA in the forceps major observed in the BD patients, might have been due to the medications used by the BD patients. In summary, the present findings show that FA values, especially in right hemisphere, can be used to differentiate SCH and BD patients. Moreover, these findings are consistent with the current understanding of the neurobiology of BD and its clinical presentation, which is characterized by substantial alteration in emotion regulation [40].

Another implication of the present study's findings is based on the fact that the study employed a hybrid approach—a supervised learning model and genetic algorithm—to differentiate SCH and BD patients. As compared to other ML methods, such as SVM and decision trees, ANNs have many advantages that must be considered by any prospective user. The ability to use multiple network architectures, learning algorithms, connections, and topologies, a computationally inexpensive structure, and flexible transfer functions are among the benefits of ANNs. Moreover, as the training process runs regardless of the size of the dataset and the relative importance of the input variables, an optimization algorithm (GA) was employed in the present study in order to select features that are more informative. The results obtained show that GA increased the overall classification accuracy with less number of features. The other measures—ROC curve, AUC, and Gini values—were implemented to determine the specific contribution of the feature selection method used. Based on the present findings, we think the ANN-GA architecture can be used as a powerful computational tool for data gathered from medical monitoring instruments and, thusly, can be applicable to clinical studies based on diagnostic findings.

The present findings also show that the SCH and BD groups differed significantly from the control group in a wide range of white matter tracts, and in many instances, the SCH and BD groups differed in a similar fashion from the control group. Previous DTI studies reported that there is substantial overlap of altered white matter tracts in SCH and BD patients [e.g., 17]. Interestingly, genetic studies also indicate that SCH and BD share a number of genetic risk factors [41]. Additional research based on genetic and imaging findings might yield more accurate methods of differentiating patients with BD and SCH.

The primary limitation of the present study is that most of the patients were on medication when MRI scanning was performed. The naturalistic design of this study may not rule out the confounding effects of medication. However, the course of chronic psychiatric conditions usually does not allow strict experimental inclusion criteria due to the long course of illness and problems in reaching unmedicated patients. As a natural limitation, the mechanism of pharmacological agents used in BD and SCH are slightly different and the effects of this issue in the brain connectivity could not be exempted. Future studies should investigate drug-naïve patients; however, as most SCH and BD patients are prescribed mood stabilizers immediately after diagnosis, it might be difficult to find such patients. Another limitation is that non-isotropic voxels were used. The normalization of non-isotropic voxels changed the voxel dimensions, which might have resulted in underestimation of FA in areas with crossing fibers [42]. To overcome this problem, an ROI-based approach might prove to be more effective than whole-brain comparison. In the present study FA values in the white matter tracts were extracted one by one in an attempt to reduce the likelihood of underestimation due to crossing fibers.

5 Conclusion

Finally, the results demonstrate that tract-based spatial statistics is a potential method used to discriminate between SCH and BD based on whole-brain analysis that relies on voxel-based comparison using nonlinear image transformation and permutation tests with correction for multiple comparisons. In addition, the ML approaches employed are useful for classifying brain abnormalities and represent a step toward development of a tool for accurately differentiating SCH and BD patients. In this context, the paper puts forward a study using two-step hybridized methodology: GA algorithm for feature selection process

and machine learning methods, namely ANN and SVM, for training process. The noteworthy performance of ANN–GA approach stated that it is possible to discriminate 36 SCH and 29 BD subjects using selected features with 81.25% overall classification accuracy. Our findings support the potential utility of the proposed methodology to be used as a clinical tool in classifying SCH and BD subjects. Further studies are warranted to replicate this result in order to lead to the development of clinically useful diagnostic methodologies and should be designed to determine the effects of medications used to treat SCH and BD on connectivity.

Compliance with ethical standards

Conflict of interest The authors certify that they have no affiliations with or involvement in any organization or entity with any financial interest (such as honoraria; educational grants; participation in speakers' bureaus; membership, employment, consultancies, stock ownership, or other equity interest; and expert testimony or patent-licensing arrangements), or non-financial interest (such as personal or professional relationships, affiliations, knowledge or beliefs) in the subject matter or materials discussed in this manuscript.

Appendix 1: Artificial neural network—supervised learning

An artificial neural network (ANN) could be described as a machine learning approach that mimics a biological nervous system, and is a powerful modeling tool for approximating nonlinear relationships and finding patterns within a dataset. An ANN is a structure used for processing information and approximating functions based on a number of inputs. With adaptive ability to be used as an arbitrary function approximation mechanism, ANNs "learn" from the observed data. Following the training process, an ANN model predicts response for any given input. That is, an ANN can be used to infer a function based on the collected input/output data. The main features of an ANN are learning adaptation, generalization, massive parallelism, robustness, and abstraction. The structure of a basic ANN can be theoretically modeled, as depicted in Fig. 4, where $X\{x_i, i = 1, 2, \ldots, n\}$ is the input matrix to the neuron and Y denotes the output of the model.

Inputs are connected to each neuron via a mathematical process. Each input is multiplied by a weight (w_i) associated with each neuron, and a constant bias (b) is added to that scalar value. The process is repeated for each input for all neurons, and finally, their sum goes through a transfer function (f) that is expressed as given in Eq. 1 [8].

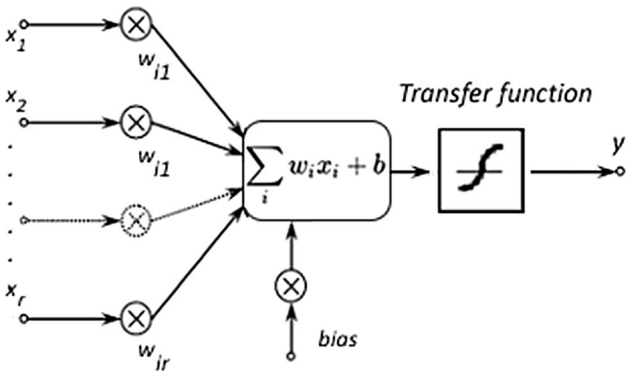

Fig. 4 Basic structure of an ANN

$$Y = f\left(\sum_{i=1}^{n} w_i x_i + b\right) \tag{1}$$

There is a wide variety of transfer functions and selection of the proper transfer function is crucial. As there is a nonlinear relationship between the input and output, nonlinear transfer functions are widely adopted for medical image processing. With selection of proper activation functions and connection of neurons, various neural networks can be constructed and trained to generate specified outputs. ANN learning paradigms for medical image processing generally include supervised learning and unsupervised learning. For supervised learning, a network is trained with preset input and output data. During the training process, a set of inputs is used to generate associated output values until the ANN output converges to the reference target with a predefined error value that is ideally zero. Accordingly, the aim of the training process is to minimize the network's overall output error for all training cases by iteratively adjusting the neuron connection weights and bias values using a specific training algorithm.

Training process

BP neural network is a typical multilayer feed-forward network trained according to backpropagation algorithm. BP neural network uses parallel distributed processing approach to handle both qualitative and quantitative knowledge. It has strong robustness, fault tolerance, and adaptability and can fully approximate any complex nonlinear relationship. Because of these advantages, BP neural network is more appropriate for processing EEG data which are possible noisy, unstable, and nonlinear. In this study, for modeling process, feed-forward neural network trained by a backpropagation algorithm is used. The network is based on the supervised procedure, i.e., the network constructs a model based on examples of data with known outputs. The architecture of the network is a layered feed-forward neural network, in which the nonlinear

elements (neurons) are arranged in successive layers, and the information flows from input layer to output layer, through the hidden layer(s). Sigmoid transfer function used in each neuron because of its nonlinear behavior. In order to minimize the error between the model output and a reference value, MSE (mean square error) is used as the cost function, given in Eq. 2. The cost function is minimized by GA.

$$J(w) = \frac{1}{N}\sum_{k=1}^{N}(y_k - z_k)^2 \tag{2}$$

The sigmoid function was used in the present study as the activation function, and TrainBR (Bayesian regularization backpropagation) was used as the training algorithm. TrainBR is a function that updates the weight and bias values according to the Levenberg–Marquardt optimization method, and minimizes a combination of squared errors and weights in order to determine the correct combinations, so that the generated model can generalize well. For the validation process, fourfold cross-validation with shuffled sampling was employed. The ANN structure was set as a multilayer perceptron (MLP)—a powerful function approximator for prediction and classification using a supervised learning algorithm. The architecture of an MLP neural network is constructed with two layers. A basic two-layer ANN contains an input layer connected to input variables and an output layer that generates the corresponding output. Although an MLP is a satisfactory approximator for linear problems, hidden layers for analyzing nonlinearity and complexity problems are added.

Appendix 2: Genetic neural network

A genetic algorithm (GA) is a very powerful meta-heuristic and evolutionary algorithm that has been used with other evolutionary algorithms for multiple problems across disciplines. Despite the advent of newly adapted meta-heuristic methods, GA remains a popular choice for solving many challenging optimization problems for exact methods that are computationally too expensive. Moreover, due to its intrinsic structure, which is similar to the use of a set (a population) of solutions to be optimized in parallel, GA is considered a natural method for solving problems with multi-objective characteristics.

GA is a stochastic approach inspired by actual genetic processes and follows the "survival of the fittest" mechanism. GA is widely used for optimizing large, complex, and multi-dimensional problems, and generating optimal solutions. The optimization process begins with a set of possible solutions obtained from the whole search space consisting of all features. Each solution is encoded by a set of string expressions (referred to as chromosomes). The set of chromosomes are considered the population. Via the optimization process shown in Fig. 5, the performance of each string is associated with an objective function that

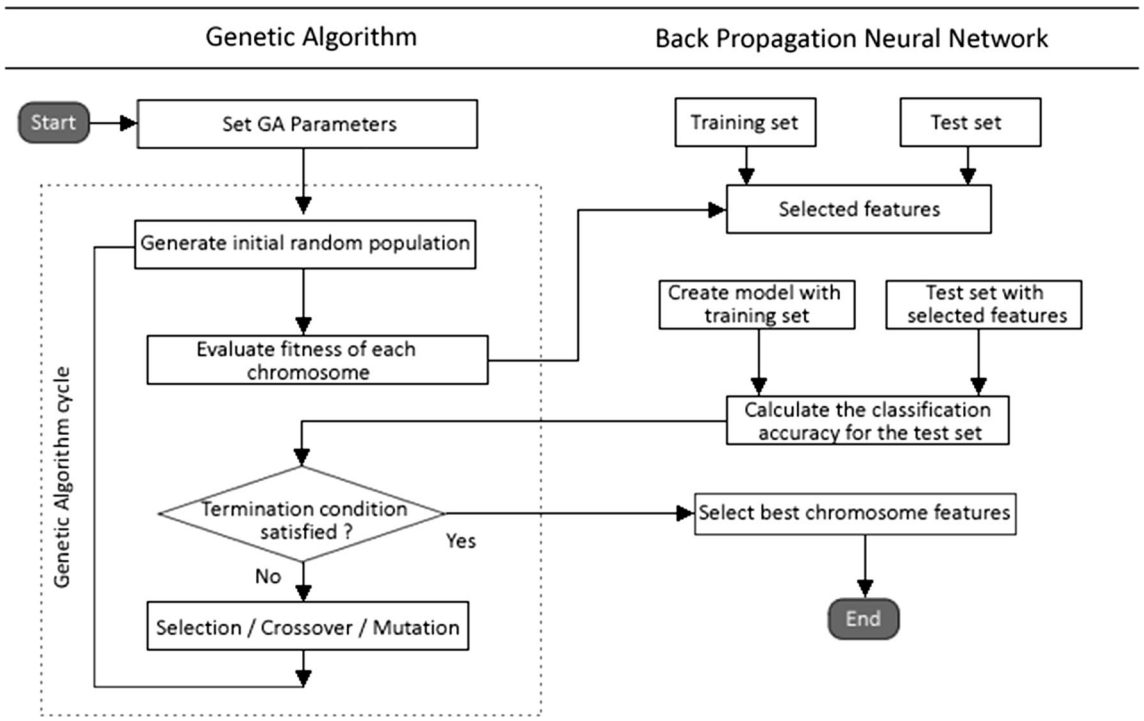

Fig. 5 Flowchart of an ANN-GA architecture

evaluates the fitness of a string for the next generation. As such, the objective function is referred to as the fitness function. Considering the fitness values of the strings, the fittest strings are selected and genetic operators, such as crossover and mutation, are applied to generate subsequent generations. This process of selection, crossover, and mutation is iteratively repeated until a maximum number of generations are performed. Therefore, with an adaptive structure GA is able to converge to the best solution (chromosome) that is either the global or the almost global optimal solution. The design process of GA is based primarily on four parameters (population size, crossover rate, mutation rate, and elitist selection), whereas the objective function is defined according the problem. Here, the objective function is taken into consideration apart from the aforementioned four features and only modification to the objective function is sufficient for changing the GA for new problems [43–46].

Fitness function of the wrapper approach

A fitness function is used to put forth the degree of goodness of selected subset. For a classification problem, if two subsets with different number of features present quite similar performance, the subset with less number of features comes into prominence. Therefore, the evaluation of fitness function regards two concerns: the classification accuracy and the number of features in the subset. In order to satisfy these concerns, the fitness function is designed in terms of both accuracy and number of features as:

$$f(x_j) = m * J(X_j) + n * (1/|X_j|) \quad (3)$$

where X_j is the subset constituted by jth chromosome, $J(X_j)$ is the classification accuracy using X_j, $|X_j|$ is the number of features of X_j, and $m \in [0, 1]$ and $n \in [0, 1]$ are the two coefficients used assign relative importance to classification accuracy and number of the selected subset parameters.

References

1. American Psychiatric Association (2013) Diagnostic and statistical manual of mental disorders (DSM-5®). American Psychiatric Publications, Washington
2. Walker J, Curtis V, Murray RM (2002) Schizophrenia and bipolar disorder: similarities in pathogenic mechanisms but differences in neurodevelopment. Int Clin Psychopharmacol 17:S11–S19
3. Hill SK, Reilly JL, Harris MS, Rosen C, Marvin RW, DeLeon O, Sweeney JAA (2009) A comparison of neuropsychological dysfunction in first-episode psychosis patients with unipolar depression, bipolar disorder, and schizophrenia. Schizophr Res 113(2):167–175
4. Berrettini WH (2000) Are schizophrenic and bipolar disorders related? A review of family and molecular studies. Biol Psychiatry 48(6):531–538
5. Abi-Dargham A, Rodenhiser J, Printz D, Zea-Ponce Y, Gil R, Kegeles LS et al (2000) Increased baseline occupancy of D2 receptors by dopamine in schizophrenia. Proc Natl Acad Sci 97(14):8104–8109
6. Jacobs D, Silverstone T (1986) Dextroamphetamine-induced arousal in human subjects as a model for mania. Psychiatr Med 16(02):323–329
7. Koreen AR, Siris SG, Chakos M, Alvir J (1993) Depression in first-episode schizophrenia. Am J Psychiatry 150(11):1643
8. Pearlson GD, Ford JM (2014) Distinguishing between schizophrenia and other psychotic disorders. Schizophr Bull 40:501–503
9. Vederine FE, Wessa M, Leboyer M, Houenou J (2011) A meta-analysis of whole-brain diffusion tensor imaging studies in bipolar disorder. Prog Neuropsychopharmacol Biol Psychiatry 35(8):1820–1826
10. Lin F, Weng S, Xie B, Wu G, Lei H (2011) Abnormal frontal cortex white matter connections in bipolar disorder: a DTI tractography study. J Affect Disord 131(1):299–306
11. Barnea-Goraly N, Chang KD, Karchemskiy A, Howe ME, Reiss AL (2009) Limbic and corpus callosum aberrations in adolescents with bipolar disorder: a tract-based spatial statistics analysis. Biol Psychiatry 66(3):238–244
12. Versace A, Almeida JR, Hassel S, Walsh ND, Novelli M, Klein CR et al (2008) Elevated left and reduced right orbitomedial prefrontal fractional anisotropy in adults with bipolar disorder revealed by tract-based spatial statistics. Arch Gen Psychiatry 65(9):1041–1052
13. Koch K, Wagner G, Dahnke R, Schachtzabel C, Schultz C, Roebel M et al (2010) Disrupted white matter integrity of corticopontine-cerebellar circuitry in schizophrenia. Eur Arch Psychiatry Clin Neurosci 260(5):419–426
14. Lee SH, Kubicki M, Asami T, Seidman LJ, Goldstein JM, Mesholam-Gately RI et al (2013) Extensive white matter abnormalities in patients with first-episode schizophrenia: a diffusion tensor imaging (DTI) stud. Schizophr Res 143(2):231–238
15. Liu X, Lai Y, Wang X, Hao C, Chen L, Zhou Z et al (2013) Reduced white matter integrity and cognitive deficit in never-medicated chronic schizophrenia: a diffusion tensor study using TBSS. Behav Brain Res 252:157–163
16. Seal ML, Yücel M, Fornito A, Wood SJ, Harrison BJ, Walterfang M et al (2008) Abnormal white matter microstructure in schizophrenia: a voxelwise analysis of axial and radial diffusivity. Schizophr Res 101(1):106–110
17. McIntosh AM, Maniega SM, Lymer GKS, McKirdy J, Hall J, Sussmann JE et al (2008) White matter tractography in bipolar disorder and schizophrenia. Biol Psychiatry 64(12):1088–1092
18. Lu LH, Zhou XJ, Keedy SK, Reilly JL, Sweeney JA (2011) White matter microstructure in untreated first episode bipolar disorder with psychosis: comparison with schizophrenia. Bipolar Disord 13(7–8):604–613
19. Jones DK, Symms MR, Cercignani M, Howard RJ (2005) The effect of filter size on VBM analyses of DT-MRI data. Neuroimage 26(2):546–554
20. Simon TJ, Ding L, Bish JP, McDonald-McGinn DM, Zackai EH, Gee J (2005) Volumetric, connective, and morphologic changes in the brains of children with chromosome 22q11. 2 deletion syndrome: an integrative stud. Neuroimage 25(1):169–180
21. Smith SM, Jenkinson M, Johansen-Berg H, Rueckert D, Nichols TE, Mackay CE et al (2006) Tract-based spatial statistics: voxelwise analysis of multi-subject diffusion data. Neuroimage 31(4):1487–1505

22. Smith SM, Jenkinson M, Woolrich MW, Beckmann CF, Behrens TE, Johansen-Berg H et al (2004) Advances in functional and structural MR image analysis and implementation as FSL. Neuroimage 23:S208–S219
23. Smith SM (2002) Fast robust automated brain extraction. Hum Brain Mapp 17(3):143–155
24. Mori S, Wakana S, Nagae-Poetscher LM, Van Zijl PCM (2006) MRI atlas of human white matter. Am J Neuroradiol 27(6):1384
25. Philippi CL, Mehta S, Grabowski T, Adolphs R, Rudrauf D (2009) Damage to association fiber tracts impairs recognition of the facial expression of emotion. J Neurosci 29(48):15089–15099
26. Catani M, De Schotten MT (2008) A diffusion tensor imaging tractography atlas for virtual in vivo dissections. Cortex 44(8):1105–1132
27. Martino J, Brogna C, Robles SG, Vergani F, Duffau H (2010) Anatomic dissection of the inferior fronto-occipital fasciculus revisited in the lights of brain stimulation data. Cortex 46(5):691–699
28. Bruno S, Cercignani M, Ron MA (2008) White matter abnormalities in bipolar disorder: a voxel-based diffusion tensor imaging study. Bipolar Disord 10(4):460–468
29. Garibotto V, Scifo P, Gorini A, Alonso CR, Brambati S, Bellodi L, Perani D (2010) Disorganization of anatomical connectivity in obsessive compulsive disorder: a multi-parameter diffusion tensor imaging study in a subpopulation of patients. Neurobiol Disord 37(2):468–476
30. Jacobson S, Kelleher I, Harley M, Murtagh A, Clarke M, Blanchard M et al (2010) Structural and functional brain correlates of subclinical psychotic symptoms in 11–13 year old schoolchildren. Neuroimage 49(2):1875–1885
31. Adler CM, Holland SK, Schmithorst V, Wilke M, Weiss KL, Pan H, Strakowski SM (2004) Abnormal frontal white matter tracts in bipolar disorder: a diffusion tensor imaging study. Bipolar Disord 6(3):197–203
32. Catani M, Jones DK, Donato R, Ffytche DH (2003) Occipito-temporal connections in the human brain. Brain 126(9):2093–2107
33. Shinoura N, Suzuki Y, Tsukada M, Katsuki S, Yamada R, Tabei Y et al (2007) Impairment of inferior longitudinal fasciculus plays a role in visual memory disturbance. Neurocase 13(2):127–130
34. Townsend J, Altshuler LL (2012) Emotion processing and regulation in bipolar disorder: a review. Bipolar Disord 14(4):326–339
35. Carlson PJ, Singh JB, Zarate CA, Drevets WC, Manji HK (2006) Neural circuitry and neuroplasticity in mood disorders: insights for novel therapeutic targets. NeuroRx 3(1):22–41
36. Frey BN, Andreazza AC, Nery FG, Martins MR, Quevedo J, Soares JC, Kapczinski F (2007) The role of hippocampus in the pathophysiology of bipolar disorder. Behav Pharmacol 18(5–6):419–430
37. Strasser HC, Lilyestrom J, Ashby ER, Honeycutt NA, Schretlen DJ, Pulver A et al (2005) Hippocampal and ventricular volumes in psychotic and nonpsychotic bipolar patients compared with schizophrenia patients and community control subjects: a pilot study. Biol Psychiatry 57(6):633–639
38. De Schotten MT, Dell'Acqua F, Forkel SJ, Simmons A, Vergani F, Murphy DG, Catani M (2011) A lateralized brain network for visuospatial attention. Nat Neurosci 14(10):1245–1246
39. Magioncalda P, Martino M, Conio B, Piaggio N, Teodorescu R, Escelsior A et al (2016) Patterns of microstructural white matter abnormalities and their impact on cognitive dysfunction in the various phases of type I bipolar disorder. J Affect Disord 193:39–50
40. Strakowski SM, DelBello MP, Adler CM (2005) The functional neuroanatomy of bipolar disorder: a review of neuroimaging findings. Mol Psychiatry 10(1):105
41. Forstner AJ, Hecker J, Hofmann A, Maaser A, Reinbold CS, Mühleisen TW et al (2017) Identification of shared risk loci and pathways for bipolar disorder and schizophrenia. PLoS ONE 12(2):e0171595
42. Oouchi H, Yamada K, Sakai K, Kizu O, Kubota T, Ito H, Nishimura T (2007) Diffusion anisotropy measurement of brain white matter is affected by voxel size: underestimation occurs in areas with crossing fibers. Am J Neuroradiol 28(6):1102–1106
43. Zhang J, Chen RH, Wang MJ, Tian WX, Su GH, Qiu SZ (2017) Prediction of LBB leakage for various conditions by genetic neural network and genetic algorithms. Nucl Eng Des 325:33–43
44. Sergeeva M, Delahaye D, Mancel C, Vidosavljevic A (2017) Dynamic airspace configuration by genetic algorithm. J Traffic Transp Eng (English edition) 4(3):300–314
45. Chowdhury B, Garai G (2017) A review on multiple sequence alignment from the perspective of genetic algorithm. Genomics 109(5–6):419–431
46. Jafari-Marandi R, Smith BK (2017) Fluid genetic algorithm (FGA). J Comput Des Eng 4(2):158–167